ARMA 13-226

SAND2013-1630C

# Analyzing the Effect of Large Pressure Changes on the Operational Stability of Large-Diameter Caverns for the Strategic Petroleum Reserve

Sobolik, S.R.

*Sandia National Laboratories, Albuquerque, New Mexico, USA*



This paper was prepared for presentation at the 47th US Rock Mechanics / Geomechanics Symposium held in San Francisco, California, USA, 23-26 June 2013.



**ABSTRACT:** This paper presents a case study of how large-scale computational analyses may be used in conjunction with site data to make recommendations for safe depressurization and repressurization of oil storage caverns in domal salt with unusual geometries and close proximity. These recommendations were developed in response to a wellbore casing failure, and further utilized to assess ongoing cavern storage operations. Two caverns at West Hackberry present such concerns due to their unusual shapes and close proximity to each other. Cavern 6 at West Hackberry has an unusual dish-like shape with a large rim around the circumference. The diameter of Cavern 6 at the ceiling ranges from 340 to 380 meters. Because of the shape of the cavern and the creep behavior of salt, Cavern 6 is prone to wellbore casing failures caused by tensile strains. In addition, Cavern 6 has a greater potential for tensile cracking of salt at the perimeter of the cavern during a period of increasing pressure, such as at the end of a workover procedure. Cavern 6 is in close proximity to Cavern 9, which is hourglass-shaped. The analyses presented here were used to develop guidance for general pressurization procedures for the operation of these two caverns.

## 1. INTRODUCTION

The U.S. Strategic Petroleum Reserve (SPR), operated by the U.S. Department of Energy (DOE), stores crude oil in 62 caverns located at four different sites in Texas (Bryan Mound and Big Hill) and Louisiana (Bayou Choctaw and West Hackberry). The petroleum is stored in solution-mined caverns in salt dome formations. The West Hackberry salt dome in the extreme southwestern corner of Louisiana, some 24 km from the Louisiana/ Texas border to the west and the Gulf of Mexico to the south [1]. It has an oil storage capacity of about $36\times10^6$ $m^3$ ($228\times10^6$ barrels) within 22 caverns, and has operated since 1980.

Two caverns at West Hackberry present cavern and well integrity concerns due to their unusual shapes and close proximity to each other. Cavern 6 at West Hackberry has an unusual dish-like shape with a large rim around the circumference. The diameter of Cavern 6 at the ceiling ranges from 340 to 380 meters. Because of the shape of the cavern and the creep behavior of salt, Cavern 6 is prone to wellbore casing failures caused by tensile strains. In addition, Cavern 6 has a greater potential for tensile cracking of salt at the perimeter of the cavern during a period of increasing pressure, such as at the end of a workover procedure. Cavern 6 is in close proximity to Cavern 9, which is hourglass-shaped.

This paper describes how large-scale computational analyses were used in conjunction with site data to make recommendations for safe depressurization and repressurization of oil storage caverns in domal salt with unusual geometries and close proximity. Two of the wells in Cavern 6 have recently been compromised. SPR operations instituted a workover procedure to allow repair of the well casing. To provide guidance to field operators, new geomechanical calculations were performed to determine the structural integrity of Cavern 6 in response to different pressurization rates and maximum pressures. These recommendations were developed in response to a wellbore casing failure, and further utilized to assess ongoing cavern storage operations after the second well failure. The intent of these calculations was to utilize high-performance geomechanical analyses to provide real-time support to field operations and assure cavern integrity.

## 2. SITE DESCRIPTION

The geological characteristics related to the West Hackberry site were first described by Whiting [2]. The updated three-dimensional models of Rautman et al. [3] used a more refined analysis of the data and produced models of the dome that differed slightly from the earlier models. The West Hackberry dome consists of the more-or-less typical geologic sequence of rocks. With increasing depth below the ground surface, initially there is roughly 480 m of soil and unconsolidated gravel, sand, and mud, followed by approximately 120 m of caprock, consisting of anhydrite and carbonate (a

conversion product of anhydrite). Generally, the upper portions of the caprock consist of the anhydrite conversion products of gypsum and dolomite, while the lower portion of the caprock is the initial anhydrite residue from the solution of the original domal material. The caprock is generally lens-shaped, tapering to thin edges toward the periphery of the dome.

The West Hackberry site consists of 22 caverns. Figures 1 and 2 show the relative locations and geometries of these caverns. SPR purchased five existing caverns in the early 1980s. These five Phase 1 caverns – Caverns 6, 7, 8, 9, and 11 – were created as early as 1946 and were used for brining and brine storage before the SPR took ownership of them in 1977. After that time, seventeen other storage caverns (numbered 101 to 117) were created over an eight-year period. The post-1981 caverns were built via solution mining, and all have a generally cylindrical shape (more specifically, frustums with the larger diameter at the top) of approximately 600 m (2000 feet) height and 30-45 m (100-150 feet) in radius. The Phase 1 caverns, however, were originally built for brine production, and thus they were constructed with less concern about the long-term stability of the cavern shape. Cavern 6 at the West Hackberry site has an unusual dish-like shape with a large rim around the circumference. The diameter of Cavern 6 at the ceiling ranges from 340 to 380 meters. It is also in close proximity to Cavern 9, an hourglass-shaped cavern. A profile view of Cavern 6 is shown in Figure 3, and a representation of Caverns 6 and 9 drawn in their full volume and proximity is shown in Figure 4. High-resolution sonar measurements performed on Cavern 6 in 1980 are listed in Table 1 along with the average and maximum ceiling spans. The sonars of Cavern 6, taken from the three different Cavern 6 wells, are in close agreement and show that the ceiling of Cavern 9 is located 70 m (230 feet) from its edge. The closest point of approach is with the lower lobe of Cavern 9, at approximately 60 m (200 feet).

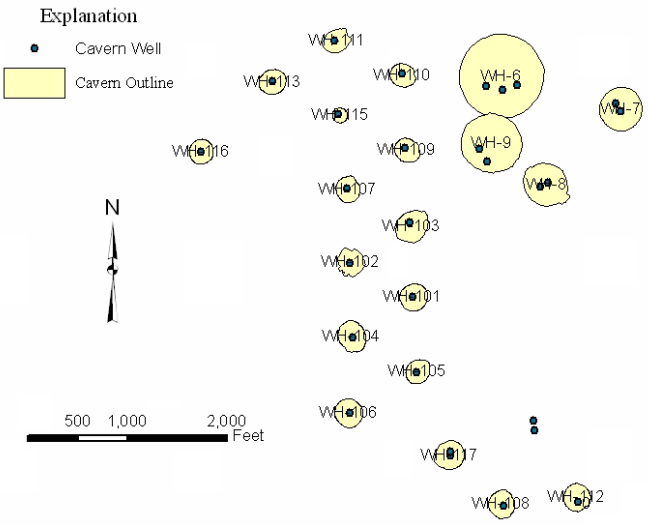


Fig. 1. Visualization of the 22 oil-storage caverns at West Hackberry SPR site viewed from the south.

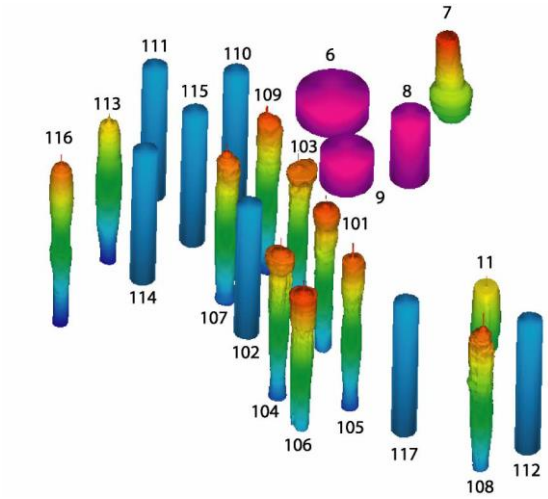


Fig. 2. Visualization of the 22 oil storage caverns at West Hackberry SPR site viewed from the southwest.

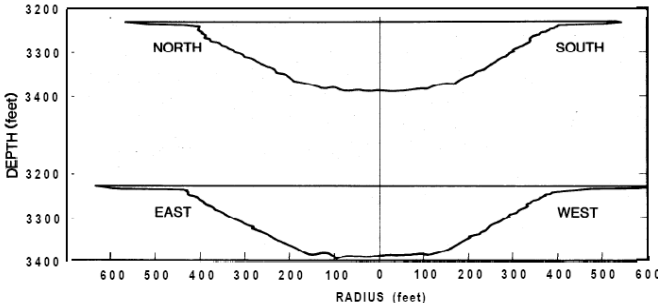


Fig. 3. Profile of Cavern 6 based on 1980-1982 sonars.

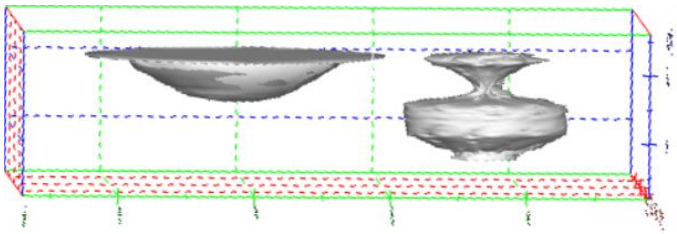

Fig. 4. Caverns 6 (left) and 9 (right), from the most recent (1982) sonar and strapping data.

Table 1. Cavern shape case summary.

| | Well | Average Ceiling Span, meters (feet) | Maximum Ceiling Span, meters (feet) |
|---|---|---|---|
| 5/21/1980 | 6 | 353.0 (1158) | 378.9 (1243) |
| 5/21/1981 | 6 | 349.0 (1145) | 375.2 (1231) |
| 3/21/1980 | 6c | 342.6 (1124) | 369.4 (1212) |
| 3/21/1980 | 6b | 344.1 (1129) | 361.8 (1187) |

When purchased in 1977, Cavern 6 had a single well, Well 6, and a 178-mm (7-inch) liner was installed down to the casing shoe prior to SPR operations. Reentry wells 6B and 6C were drilled in 1978 [4]; these wells were each constructed with a 340-mm (13.375-inch) steel casing cemented down to the casing shoe. A leak was detected in Well 6C in 1988, and a 244-mm (9.625-inch) steel liner insert was installed and cemented in 1990. Well 6B experience a leak in 2001, at a depth of approximately 686 meters (2250 feet). The leak in 6B

was repaired with an inserted liner in 2002. These casings are more prone to leakage than the casings for the other caverns at West Hackberry due to the large diameter-to-height ratio of Cavern 6.

Mechanical analyses of the West Hackberry site [5, 6] indicated that the dish-like shape of Cavern 6 make it prone to significant subsidence during normal operations, much larger than for normal-shaped caverns, which causes greater axial strain in the casings within the salt dome, particularly during workovers. Also, the cavern may potentially be at risk of dilatant and tensile damage around the cavern perimeter during repressurization after a workover. Additional concerns regarding Cavern 6 include the effect of stress changes and cracking in its vicinity on nearby Cavern 9, and the potential loss of access of oil at the perimeter of the cavern due to the deflection of the ceiling.

## 3. WELLBORE EVENTS AT CAVERN 6

Recent problems with the integrity of wells at Cavern 6 have led to workovers of the cavern for wellbore remediation. The two recent wellbore events are described below. Because of concerns of potential tensile cracking around the perimeter of Cavern 6 upon repressurization, several new sets of calculations were performed on West Hackberry in 2010 [7]. The calculations modeling the workover of Cavern 6 resulted in operational guidance to the SPR that permitted increasing the pressure quickly to an intermediate value to minimize storage loss, and then slowly increasing the pressure to a maximum operating pressure. Additional calculations were performed to simulate a workover in Cavern 9 three months after the completion of the Cavern 6 procedure, and to simulate the effect of operating Caverns 6 and 9 as a gallery (i.e., pressure changes performed simultaneously). The results of these calculations were used again after the second event in 2012 to determine a long-range strategy for the monitoring and maintenance of Cavern 6.

### *3.1. Description of September 2010 Event at West Hackberry Cavern 6*

Prior to the events of September 2010, Cavern 6 had three cemented and cased wells, two of which also had liners due to earlier well failures. At that time, a well failure occurred in the remaining unlined Well 6. The 178-mm (7-inch) production casing was logged using a Multi-Sensor Caliper as part of an ongoing program to determine the condition of SPR wellbores. The caliper survey run on August 23, 2010 and confirming camera images taken on September 1, 2010 provided compelling evidence of parted casing and severe deformation within the Well 6 cased wellbore, particularly at depths of approximately 59 and 777 meters (195 and 2,550 feet subsurface). Figure 5 shows some images of the damaged wellbore. The damage was a result of tensile strains generated along the axis of the wellbore due to cavern creep and subsidence.

The decision was made to plug and abandon the damaged well. The process required an extended workover period. The wellhead pressure was reduced to atmospheric starting on September 28, 2010, and cementing the wellbore to the Bradenhead Flange was not achieved until January 5, 2011. The geomechanical simulations described in this paper (and also in [7]) were used to develop a repressurization process that would prevent tensile cracking around Cavern 6.

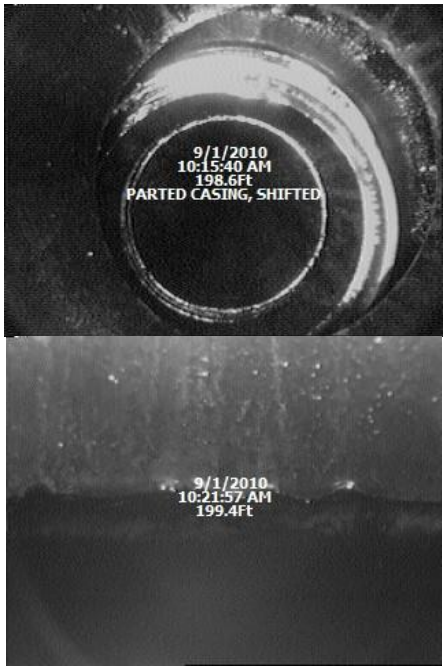


Figure 5. Camera shots showing parted casing (top: looking down well, bottom: sidewall image) just above collar at 60.8 m (199.5 feet) (courtesy DM Petroleum Operations Co.).

### *3.2. Description of May 2012 Event at Cavern 6*

As previously stated, Well 6C had experienced a failure in 1988, and a 244 mm (9.625-inch) liner was installed in 1990 to repair the wellbore. Well 6 had been plugged in early 2011, and Well 6B had been repaired in 2002. In May 2012, cavern pressure data indicated that a leak had occurred in Cavern 6. The wellhead pressure was reduced to zero, and it was discovered that Well 6C had failed in several locations. Over the next few months, as Cavern 6 was kept in workover mode, the natural pressurization rate due to creep observed in Cavern 9 had increased substantially. This elevated pressure increase in Cavern 9 raised a question about what happens if a workover on Cavern 9 is started within one year after depressuring Cavern 6 (which had previously been recommended against occurring). Because the salt around the rim of Cavern 6 (assuming the rim still exists) would still be in the process of changing back to pre-workover values, the analyses predicted that a workover in Cavern 9 could cause tensile or highly

dilatant stress values in that recovering salt, potentially causing crack propagation from Cavern 6 toward Cavern 9. Additionally, the long-term workover in Cavern 6 exacerbates the existing problems of substantial vertical strain on the casing in Well 6B, and the additional loss of access to oil in the cavern due to ceiling subsidence.

## 4. RESULTS OF EARLIER ANALYSES

Prior to the 2010 event, an earlier set of analyses was performed of the mechanical behavior of the caverns at the West Hackberry site [5]. These analyses indicated several concerns about Caverns 6 and 9:

- Because of the dish-like shape of Cavern 6, the perimeter of the cavern is at risk of dilatant and tensile damage, particularly at the end of a workover operation.
- Because of tensile cracking potential near Cavern 6, the close proximity of Cavern 9 (60 meters at their closest point) poses a risk of inter-cavern communications. The potential exists for a crack to propagate from Cavern 6 and intersect Cavern 9, causing cavern pressures to equilibrate. An operational scenario of having Cavern 9 in workover mode during the breach would pose a serious risk to operational safety and containment of oil. A breach when Cavern 6 is fully repressurized (the most likely condition) could abruptly pressurize Cavern 9 and potentially result in oil loss in the absence of a wellhead or if the blowout preventer faulted. This could pose a safety risk to the workover crew and potential environmental damage.
- Cavern 9 has a middle section with a smaller radius, giving a cross-section of the cavern the look of a bell with a mid-cavern ledge. This ledge and the cavern wall underneath supporting the ledge are also locations with a significant potential for dilatant damage during workover operations.
- Workovers performed on Cavern 9 wells should be performed no sooner than one year after the completion of a workover in Cavern 6. This period will allow the stressed salt around Cavern 6 enough time to heal and attain near-hydrostatic stress values, so to minimize the possibility of cracking the salt between Caverns 6 and 9. Performing the workovers in the opposite order (Cavern 9, then Cavern 6) does not appear to need such a stringent requirement, although it may be prudent to keep the same delay.

Because of the results of these previous analyses, the SPR site office was already sensitive to the potential integrity issues regarding Cavern 6. Therefore, in response to the decision by the SPR site office to initiate a workover on Cavern 6, a new set of calculations was performed to develop recommendations for the repressurization of the cavern. These analyses were performed with the same computational mesh, boundary conditions, and cavern operating conditions as the [5] analyses, but with greater detail given to the rate of repressurization, and with an improved material model for the salt.

## 5. DESCRIPTION OF THE MODEL

Following the September 2010 event, a series of several large-scale simulations of the West Hackberry site were performed to understand the effects of repressurization of Cavern 6 at various rates on cavern stability [7]. These calculations utilized JAS3D, Version 2.0.F [8], a three-dimensional finite element program developed by Sandia National Laboratories, and designed to solve large quasistatic nonlinear mechanics problems. Several constitutive material models are incorporated into the program, including models that account for elasticity, viscoelasticity, several types of hardening plasticity, strain rate dependent behavior, damage, internal state variables, deviatoric creep, and incompressibility. The continuum mechanics modeled by JAS3D are based on two fundamental governing equations. The kinematics are based on the conservation of momentum equation, which can be solved either for quasistatic or dynamic conditions (a quasistatic procedure was used for these analyses). The stress-strain relationships are posed in terms of the conventional Cauchy stress.

Historically, three-dimensional geomechanical simulations of the behavior of the caverns at SPR facilities had been performed using a power law creep model, which evaluates only the secondary steady-state salt creep mechanism. Because the transient creep mechanism is not represented in this model, the common practice has been to use a reduction factor for the elastic modulus. Using this method, and calibrating the creep coefficient to field data such as cavern closure and surface subsidence, analysis agreement with observed phenomena has ranged from adequate to very good, depending upon the degree of homogeneity at a particular site. However, the power law creep model used in this manner is not well suited for modeling short-term events such as pressure changes due to a workover. The artificially low elastic modulus causes an overestimation of the deformation response to depressurization and repressurization, and also incorrectly models the stress equilibration response of the salt after such an event.

In 2010, enhancements were completed to the integration algorithm within the model to create a more stable implementation of the multi-mechanism deformation (M-D) model [6]. The M-D model is a rigorous mathematical description of both transient and steady-state creep phenomena. It was originally developed by Munson and Dawson [9, 10, 11], and later extended

[12]. This constitutive model considers three well-recognized fundamental features of a creeping material: a steady-state creep rate, a transient strain limit, and both a work-hardening and recovery time rate of change (i.e. curvature). Because of the highly nonlinear nature of the curvature of the transient strain response, this model has been difficult to integrate in a fully three-dimensional calculation for a model with hundreds of thousands of elements. Many published papers exist presenting two-dimensional calculations using the M-D model, but three-dimensional, large-scale simulations have been more difficult due to the model's high nonlinearity. Full descriptions of the M-D model and the integration algorithm enhancements are provided in [6].

The computational domain developed for [5] and [6] for the West Hackberry cavern field encompasses the eastern half of the salt dome, with a vertical symmetry plane through six WH caverns (110, 109, 103, 101, 105, and 117). The mesh for the computational model is illustrated in Figures 6 and 7. Figure 6 shows the entire mesh used for these calculations, and Figure 7 shows the same view with the overburden and caprock removed to expose the salt formation. The mesh comprised 1.29 million hexagonal elements. Four material blocks were used in the model to describe the stratigraphy: the overburden, caprock, salt dome and sandstone surrounding the salt dome. The overburden is made of sand, and the caprock layer is made of gypsum or limestone. Figure 8 shows two views of the layout of the meshed caverns used for these calculations, which includes the six half caverns listed above, which are spaced approximately 230 m (750 feet) center-to-center, plus full cavern representations for 108 and the Phase 1 caverns (6, 7, 8, 9, and 11).

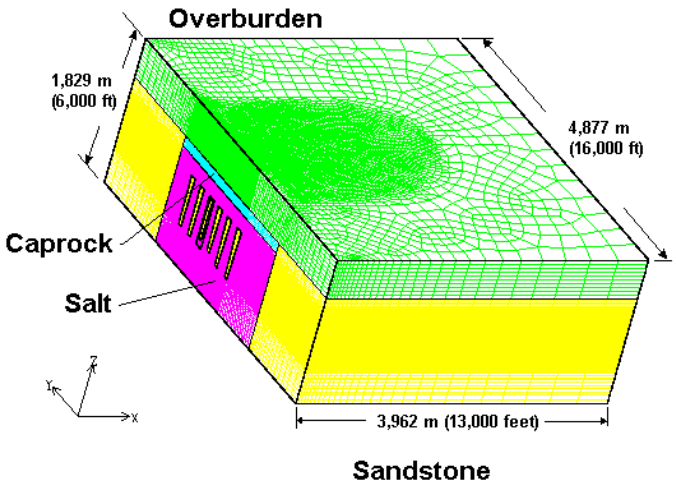


Fig. 6. Computational mesh used for the West Hackberry calculations.

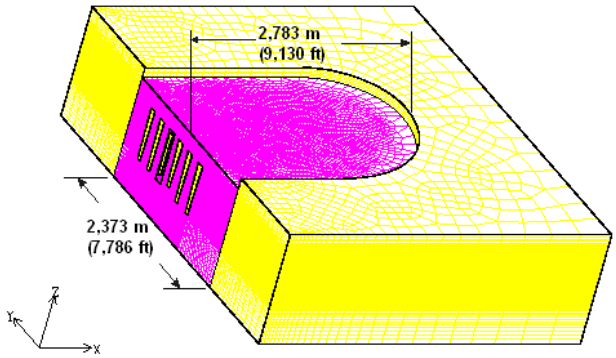


Fig. 7. Computational mesh showing the salt formation and surrounding sandstone.

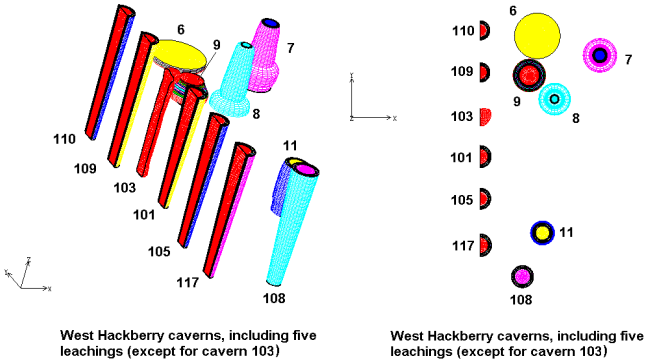


Fig. 8. West Hackberry caverns included in the computational mesh (two views).

The parameters used for the M-D model are listed in Table 2. The properties were developed from [13], which includes properties for SPR salts developed from a combination of laboratory tests on SPR salt samples and other property values developed from WIPP salt. The analyses described in [6] comprised an extensive computational effort to develop a set of M-D properties that, when used with the computational mesh would produce predictions of surface subsidence and cavern closure that would satisfactorily match West Hackberry site data. The analyses in [6] showed predictions with three sets of M-D properties, and found that using the M-D properties for West Hackberry in [13], with a multiplier of 1.7 applied to the transient strain limit coefficient $K_0$, provided an excellent match for the subsidence and a very good match for the cavern closure data. For later analyses described in [7] and in this paper, a multiplier of 1.2 was used instead; this multiplier provided a better match for cavern closure data with very little loss of accuracy for surface subsidence predictions.

The use of the M-D model provided an improved modeling of the effect short-term pressure transients on cavern behavior. However, the M-D model did increase the computational CPU time for the 85-year simulation over a similar calculation using the power law creep

model by approximately 60%, from ~36 CPU hours to about ~60 hours using 32 processors in parallel. Nevertheless, the gain in temporal discretization of short-term pressure transients far outweighs the inconvenience of more CPU time consumption.

Table 2. M-D Model mechanical properties used for West Hackberry salt.

| Property | West Hackberry, soft salt properties |
|---|---|
| Density, kg/m$^3$ | 2300 (144 lb/ft$^3$) |
| Elastic modulus, GPa | 31.0 (4.50 ×10$^6$ psi) |
| Shear modulus G, GPa | 12.4 (1.80 ×10$^6$ psi) |
| Poisson's ratio | 0.25 |
| Primary Creep Constant $A_1$, sec$^{-1}$ | 9.81 ×10$^{22}$ |
| Exponent $n_1$ | 5.5 |
| $Q_1$, cal/mol | 25000 |
| Secondary Creep Constant $A_2$, sec$^{-1}$ | 1.13 ×10$^{13}$ |
| Exponent $n_2$ | 5.0 |
| $Q_2$, cal/mol | 10000 |
| $B_1$, sec$^{-1}$ | 7.121×10$^6$ |
| $B_2$, sec$^{-1}$ | 3.55×10$^{-2}$ |
| $\sigma_0$, MPa | 20.57 (2983 psi) |
| q | 5335 |
| m | 3.0 |
| $K_0$ | 7.53×10$^5$ |
| c | 0.009198 |
| α | -17.37 |
| β | -7.738 |
| δ | 0.58 |

## 6. RESULTS

### *6.1. Analysis for the 2010 Workover on Cavern 6*

The 1980 sonar data from Cavern 6 indicate that the approximately 60-m (200-feet) wide "rim" encircling the cavern has been present since at least 1980, and was about 10 feet thick at the edge of the dish or bowl portion of the cavern. Unfortunately, the 1981 sonar measurements are the last data taken of the cavern profile. The current condition of the rim of Cavern 6 is not known. This may be important for two reasons. One, the extension of the flat wide volume of the cavern may increase the already high fracture potential around the perimeter, and consequently cause the cavern ceiling to subside more. Two, because of the geometry of the cavern, it is possible that the rim has been pinched off from the rest of the cavern, potentially trapping oil in the pinched section or in pockets near the rim that are at higher elevations than the access holes in the cavern ceiling. Therefore, there are three probable current conditions of the rim around Cavern 6:

- The rim is highly compressed, but there is still enough oil in it to allow pressure communication from the main cavern out to the edge of the rim;
- The rim is completely pinched off at the edge of the main part of the cavern, meaning there is in essence no more rim; or
- The rim is pinched off somewhere between the main cavern and the original rim edge.

Mechanical simulations were performed with JAS3D and the M-D model assuming either communication with the edge of the rim, or that the rim no longer exists. The analyses were identical to those performed for [5], except that the M-D model was used instead of the power law creep model, and the pressure changes during the workover period for Cavern 6 were altered. For all the analyses, the wellhead pressure in Cavern 6 was dropped from its normal operating pressure of 6.2 MPa (900 psi) to 0 MPa for the workover in 120 hours (5 days), and then held at 0 MPa for an additional 55 days before repressurization. Five sets of calculations were performed:

- Cavern with rim, raise wellhead pressure from 0 to 6.2 MPa (900 psi) in 24 hours (1 day).
- Cavern with rim, raise wellhead pressure from 0 to 6.2 MPa (900 psi) in 72 hours (3 days).
- Cavern with rim, raise wellhead pressure from 0 to 6.2 MPa (900 psi) in 120 hours (5 days).
- Cavern with a closed rim, raise wellhead pressure from 0 to 6.2 MPa (900 psi) in 72 hours (3 days).
- Cavern with rim, with a staged repressurization: raise wellhead pressure from 0 to 4.8 MPa (700 psi) in 72 hours (3 days), followed by a seven-day period raising the pressure to 5.9 MPa (850 psi).

Figure 9 shows the maximum stress around the perimeter of the cavern during repressurization. For the simulations that assume communication with the edge of the rim still exists, the maximum stress is at the edge of the rim; for the case with a closed rim, the stress occurs at the perimeter of the main bowl of the cavern. The "x" on each curve indicates when each simulation reaches 4.8 MPa (700 psi) wellhead pressure. Note that for the three cases with a rim and a steady repressurization, the maximum stress becomes tensile when the wellhead pressure reaches its maximum simulation pressure of 6.2 MPa. Note also that there is some improvement as the repressurization period increases. For the case with a closed rim, the maximum stress nears but does not become tensile at its maximum wellhead pressure. This result is significant, because the corresponding results using the power law creep model in [5] indicated that tensile stresses would occur during this process; the M-D model, which handles transient stress effects more realistically, shows that tension should not occur, although the predicted stresses come uncomfortably close to tension. For the case of the staged repressurization, the maximum stress reaches its maximum value of 2.1 MPa in compression at 10 days and 5.9 MPa wellhead pressure, and then begins to re-

equilibrate to in situ stress. These results indicate that the best approach for repressurization is to relatively quickly (i.e. in 3 days) increase the wellhead pressure to 4.8 MPa to mitigate further storage capacity loss, then take a much longer time (at least seven days) to increase the wellhead pressure to the minimum of the normal operating range or 5.9 MPa. Figure 10 shows the resulting stress re-equilibration for up to 450 days after the end of the workover. Note that the maximum stress has not reached the in situ value before the end of the analysis at 450 days. Because of the proximity of Cavern 9, this result would seem to reinforce the recommendation to wait at least one year between workovers of Caverns 6 and 9.

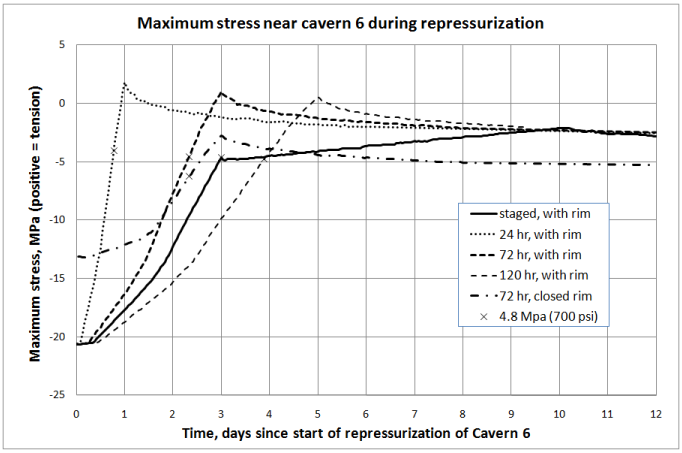


Fig. 9. Maximum stress around Cavern 6 during repressurization.

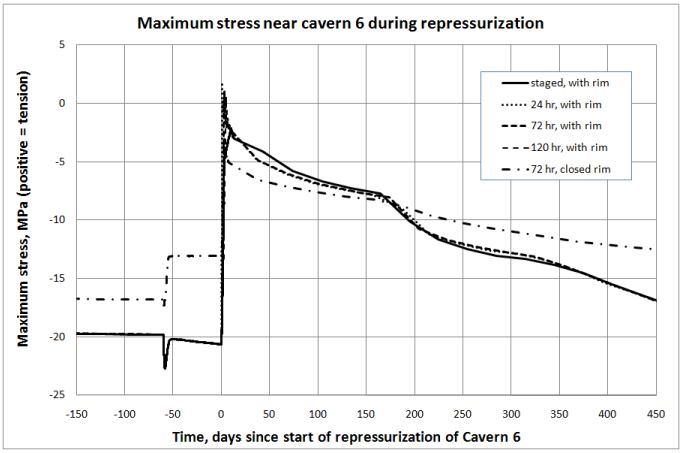


Fig. 10. Maximum stress around Cavern 6 over a year after repressurization.

The damage factor used in this study is identified by a dilatant damage criteria defined by a linear function relating shear stress to hydrostatic pressure. Dilatancy is considered the onset of damage to rock resulting in significant increases in permeability. Dilatant damage in salt typically occurs at the point at which microfracturing initiates, resulting in volume increase. Dilatant criteria typically relate two stress invariants: the first invariant of the Cauchy stress tensor $I_1$ (equal to three times the mean stress) and the square root of the second invariant of stress deviator $J_2$, or $\sqrt{J_2}$ (a measure of the overall deviatoric or shear stress). One dilatant criterion is the linear equation typically used from [14],

$$\sqrt{J_2} = 0.27 I_1 . \quad (1)$$

This damage criterion defines a linear relationship between $I_1$ and $\sqrt{J_2}$, and such linear relationships have been established from many suites of lab tests on WIPP, SPR, and other salt samples. (More typically, the relationship between $I_1$ and $\sqrt{J_2}$, is exponential and asymptotically approaches a linear relationship as described in Equation 1. This criterion is used in lieu of laboratory dilatancy data specifically derived from West Hackberry salt samples.) This criterion was applied during post-processing of the analyses. A damage factor index was defined for this criterion (DF) by normalizing $\sqrt{J_2}$ from Equation 1 by $\sqrt{J_2'}$ yielding:

$$DF = \frac{0.27 I_1}{\sqrt{J_2'}}, \quad (2)$$

where $J_2'$ is the value of the second invariant of the stress deviator tensor predicted from the simulation at every point in the mesh. Several earlier publications define that the linear damage factor DF indicates damage when DF=1, and failure when DF≤0.6. This report will use these damage thresholds.

The minimum safety factors typically occur during the workover periods, when the pressure at the wellhead is reduced to 0 MPa. When the minimum safety factor in the salt is plotted as a function of time, observations can be made regarding the change in safety factor as the initial cavern radius is increased, and as a function of time. Figure 11 shows the minimum value of dilatant damage factor obtained for each of the five simulations. A value of 1 indicates the onset of dilatant damage; typically, it is desired to keep the damage factor above 1.5. As in the case of maximum stress (Figure 9), the minimum damage factor occurs at the edge of the rim, or for the case of the closed rim, at the perimeter of the main bowl of the cavern. For the three cases with a rim and steady repressurization, the damage factor drops below 1, indicating the onset of damage. Fortunately, when the pressure increase ends, stress equilibration begins immediately and the damage factor rises back above 1 very quickly. For the case of no rim, the damage factor briefly drops below 1.5 at the maximum wellhead pressure, and then recovers. This result also differs from the result using the power law creep model, which predicted a damage factor below 1 for the same cavern geometry. For the case using staged repressurization, a minimum value of the damage factor of 1.34 is reached shortly after the maximum wellhead pressure is achieved

at 10 days. This result demonstrates that at least seven days should be allowed to increase the wellhead pressure from 4.8 to 5.9 MPa.

The results presented here show that the pressure in Cavern 6 can be raised reasonably quickly to 4.8 MPa. This will help to minimize storage volume loss due to creep. Then a much slower pressure rise is warranted to prevent damage to the salt around the cavern. This repressurization process has not been violated by previous workovers for Cavern 6; Figure 12 shows historic repressurization data from previous workovers along with the current recommended limit to re-pressurize.

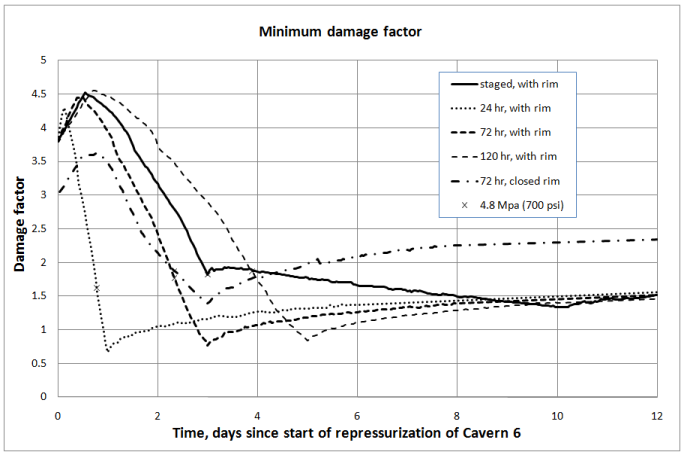


Fig. 11. Minimum dilatant damage factor around Cavern 6 during repressurization.

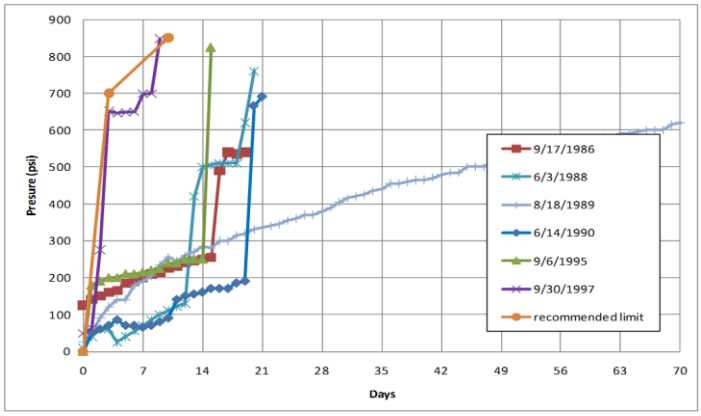


Fig. 12. Repressurization histories following previous workovers of Cavern 6.

As these calculations and others have shown, the primary causative mechanism of the well failures at SPR sites is subsidence induced by ground strains along the axis of the wellbore due to salt creep and cavern closure. These calculations also demonstrated that following a workover in Cavern 6, repressurization of the cavern must be performed slowly to avoid tensile fracturing at the roof. Based on these results, it was recommended to DOE that the wellhead pressure in Cavern 6 be re-pressurized to 4.8 MPa (700 psi) over three days, followed by an additional seven-day period (minimum; longer would be better) to raise the wellhead pressure to 5.9 MPa (850 psi). The initial and more rapid pressure increase would help mitigate creep closure losses in the cavern. The subsequent and more sensitive pressure rate must be slower to avoid tensile fracturing at the edge of the large flat diameter roof.

Following the completion of wellbore cementing on January 5, 2011, the repressurization of the cavern started on January 14, 2011 and lasted throughout January following the recommendations in this report. The wellhead pressure in Cavern 6 was raised to 4.8 MPa (700 psi) over three days, followed by an additional fourteen-day period to raise the wellhead pressure to the low end of its normal operating range, 5.9 MPa (850 psi) on January 31, 2011. Based on all indications from well pressure measurements from Caverns 6 and 9, there was no evidence of additional well damage or loss of cavern integrity until May 2012, indicating that the prescribed repressurization rate was not excessive.

### *6.2. Application of Results to the 2012 Well Failure Event*

As described in [5], vertical well strains in the locations of the original (c. 1946) and newer (c. 1981) wells providing access to the Phase 1 caverns in some cases have already exceeded established thresholds for cement failure (0.2 millistrains) and steel casing collapse (1.6 millistrains). In particular the greatest strain was predicted above Cavern 6 with yielding predicted in the 2000-2002 timeframe. This prediction was validated with the failure of Well 6B in 2001, requiring the installation of a liner in 2002. After the well failure in Well 6C in May 2012, concerns were raised about the condition of Well 6B, now the only operational well for Cavern 6. The most recent calculations [7], using the M-D model, confirmed the previous predictions, and indicated that although the strain rate on the casing is not excessive during normal operations, it is significantly higher during depressurization such as a workover. Figure 13 shows the resulting vertical strain as a function of depth during a workover on Cavern 6. The maximum strains occur between 2500 and 2700 feet (760-823 m) depth, which corresponds to the location of the 2010 failure in Well 6. At this location, as much as 0.9 millistrains may be added to the existing strain imposed on the casings. This value is over half the threshold for steel. If the steel is already in or near plastic deformation, the additional strain imposed during a workover may cause failure in the casing due to fracture, collapse, or thread jumping at the joints.

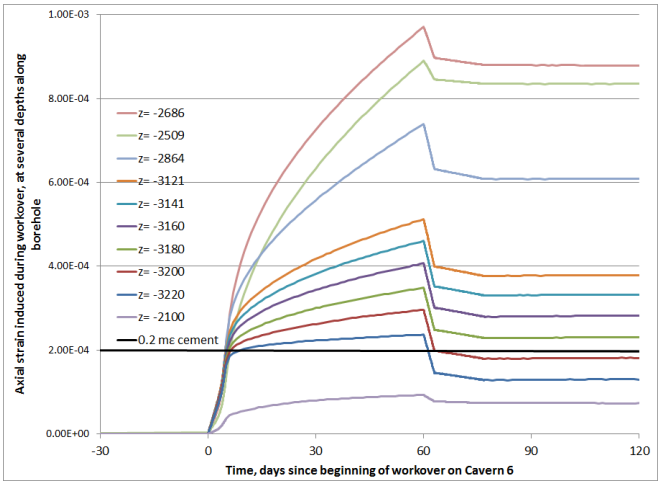


Fig. 13. Axial well strain for Cavern 6 during a workover, at several locations above the ceiling.

Figure 13 indicates that well casings in the Cavern 6 wells will need to be remediated every 2 to 3 workover cycles. Because of the large ceiling of Cavern 6, axial strains large enough to cause failure of the casings due to thread jumping at the joints or plastic failure of the steel casings are expected to occur on a regular basis, perhaps every 10-20 years, and particularly during low pressure periods such as workovers. Well 6B has experienced two workovers in the span of two years, and thus may be near failure conditions once again. Because of this, continued operation of Cavern 6 as an oil storage cavern should require the operator to be prepared to replace the casings for the cavern regularly, or to drill additional wells into the cavern. This condition would continue to be a concern if Cavern 6 is abandoned for oil storage, in that the replacement fluid (brine) may need to be pressurized to maintain low strain rates.

The large ceiling of Cavern 6 has dropped over the three decades since oil storage began. As the ceiling has dropped, it has likely caused the wellbore opening to drop below the levels of the outer rim of the cavern, and much of the interior of the cavern as well. Because of this, oil recovery by standard brine replacement would not be possible for a significant volume of the cavern. Based on the geomechanical calculations of [7], crude estimates were developed of the amount of oil that may be currently or may become inaccessible are based on the cavern geometry from the 1980 sonar (which includes a large outer rim of up to 620 feet radius and an originally flat ceiling). The current condition of the outer rim of Cavern 6 is not known, but based on the 1980 sonar readings of its radius and thickness, it originally contained approximately $160\times10^3$ $m^3$ ($1\times10^6$ barrels) of oil. In addition, the middle of the cavern has (according to the geomechanical calculations) dropped about 3.1 m (10 feet) since 1982, potentially making another $48\times10^3$ $m^3$ ($0.3\times10^6$ barrels) of oil inaccessible. The ceiling is predicted to drop about 3 cm (0.1 feet) per year during non-workover years, resulting in the loss of accessibility of another 560 $m^3$ (3500 barrels) per year. During workovers on Cavern 6, that number rises significantly; the ceiling can drop 0.15-0.25 m (0.5-0.8 feet) during a 60-day to 90-day workover, making up to another 4000 $m^3$ (25,000 barrels) inaccessible. This potential rate of accessibility loss is not so severe to require immediate action; however, it will continue as long as the cavern is in service. This conclusion suggests the need to develop a long-term strategy for how to access and remove currently inaccessible oil from the cavern; such possibilities may include using pressurized nitrogen to lower the oil level in the cavern, or to drill an additional well nearer to the perimeter to allow more direct access.

Because of the issues regarding the wells at Cavern 6, the Cavern Integrity Working Group for the SPR West Hackberry site (including staff from the DOE SPR management team, DM Petroleum Operations Co., and Sandia) entered into a process to evaluate the long-term disposition of Cavern 6. The driving scenarios regarding the future use of Cavern 6 are well stability and oil accessibility; cavern stability, in the form of potential dilatant and tensile fracturing around the cavern, is a high but manageable concern. Based on the recent failure of the other two wells at Cavern 6, and on geomechanical calculations, Well 6B is determined to already be at a high risk of failure, and dropping the pressure in the cavern increases that risk. If Well 6B is lost (either in normal operations or during a workover), then the $0.95\times10^6$ $m^3$ ($6\times10^6$ barrels) of oil in the cavern will become inaccessible until another well is drilled. Based on these conclusions, the working group recommended emptying as much oil as possible from Cavern 6 using brine, then performing post-removal diagnostics, including a sonar scan of the cavern to map the ceiling and also estimate how much oil remains in the cavern. (The ceiling map will help to plan for the long-term pressure maintenance of this cavern with brine or some other substance.) Diagnostics will also include a multi-arm caliper to evaluate well deformation. During and after these operations, the Working Group will weigh the pros and cons of maintaining Cavern 6 for oil storage versus decommissioning, using the acquired geotechnical data and cost/benefit analyses. Decommissioning means the permanent removal of accessible oil from Cavern 6, and long-term pressure maintenance (with brine or some other fluid) and monitoring of the cavern. The oil removal process was begun on February 1, 2013.

## 7. CONCLUSIONS

The computational model for the West Hackberry SPR site presented here is mature, with a mesh containing realistic geometries for the caverns and salt dome, a functional M-D model, and operating pressure scenarios that can be modified to fit current and new scenarios.

Previous analyses with this model have been able to predict the well failures that occurred in the field, such as the well failure in Cavern 6. The analysis presented in this report demonstrates the capability to apply complex, three-dimensional geomechanical computations to make recommendations to field operations in a short time frame. The recommended procedure insured a safe repressurization of Cavern 6, and there has been no event indicative of loss of cavern integrity since the workover was completed. The results of the analyses were later used in response to a second well failure to anticipate potential problems that may occur with Cavern 6 and its one existing operational well, and plan operational procedures to prevent or mitigate negative consequences. Based on these results, a process has begun to remove oil from the large-diameter cavern to allow for inspection of the cavern, to estimate the amount of oil made inaccessible by cavern deformation, and to evaluate the future integrity of the cavern and its wells. After a rigorous inspection of Cavern 6, a future decision will be made regarding whether the cavern is still acceptable for oil storage purposes, or whether the cavern must be decommissioned and filled with brine for the purposes of enhancing the continued safe storage of oil in nearby Cavern 9.

## 8. ACKNOWLEDGEMENTS

Sandia National Laboratories is a multi-program laboratory managed and operated by Sandia Corporation, a wholly owned subsidiary of Lockheed Martin Corporation, for the U.S. Department of Energy's National Nuclear Security Administration under contract DE-AC04-94AL85000.

## REFERENCES

1. Munson, D.E., 2006. *Features of West Hackberry Salt Caverns and Internal Structure of the Salt Dome*, SAND2006-5409, Sandia National Laboratories, Albuquerque, New Mexico.
2. Whiting, G. H., 1980. *Strategic Petroleum Reserve (SPR): Geological Site Characterization Report, West Hackberry Salt Dome*, SAND80-7131, Sandia National Laboratories Albuquerque, New Mexico.
3. Rautman, C.A., J.S. Stein, and A.C. Snider, 2004. *Conversion of the West Hackberry Geological Site Characterization Report to a Three-Dimensional Model*, SAND2004-3981, Sandia National Laboratories, Albuquerque, New Mexico.
4. McHenry, J.A., 2001. *Cavern Integrity Test Report – West Hackberry Cavern WH-6*. Prepared for Strategic Petroleum Reserve, Publication No. WHE7000.609A0.
5. Sobolik, S.R. and B.L. Ehgartner, 2009. *Analysis of Cavern Stability at the West Hackberry SPR Site*. SAND2009-2194, Sandia National Laboratories, Albuquerque, New Mexico.
6. Sobolik, S.R., J.E. Bean, and B.L. Ehgartner, 2010. Application of the Multi-Mechanism Deformation Model for Three-Dimensional Simulations of Salt Behavior for the Strategic Petroleum Reserve. In *Proceedings of the 44th US Rock Mechanics Symposium and 5th U.S.-Canada Rock Mechanics Symposium, Salt Lake City, UT June 27–30, 2010*, ARMA No. 10-403.
7. Sobolik, S.R. & B.L. Ehgartner, 2012. Analyzing Large Pressure Changes on the Stability of Large-Diameter Caverns Using the M-D Model. In *Mechanical Behavior of Salt VII: Proceedings of the 7th Conference on the Mechanical Behavior of Salt, Paris, France, 16-19 April 2012*, eds. Berest, Ghoreychi, Hadj-hassen & Tijani, 321-330. London: CRC Press, Taylor & Francis Group.
8. Blanford, M.L., M.W. Heinstein, & S.W. Key, 2001. *JAS3D. A Multi-Strategy Iterative Code for Solid Mechanics Analysis. User's Instructions, Release 2.0.* SEACAS Library, JAS3D Manuals, Computational Solid Mechanics / Structural Dynamics, Sandia National Laboratories, Albuquerque, NM.
9. Munson, D.E. and P.R. Dawson, 1979. *Constitutive Model for the Low Temperature Creep of Salt (With Application to WIPP).* SAND79-1853, Sandia National Laboratories, Albuquerque, New Mexico.
10. Munson, D.E. and P.R. Dawson. 1982. *A Transient Creep Model for Salt during Stress Loading and Unloading.* SAND82-0962, Sandia National Laboratories, Albuquerque, New Mexico.
11. Munson, D.E. and P.R. Dawson, 1984. Salt Constitutive Modeling using Mechanism Maps. *1st International Conference on the Mechanical Behavior of Salt, Trans Tech Publications*, 717-737, Clausthal, Germany.
12. Munson, D.E., A.F. Fossum, and P.E. Senseny. 1989. *Advances in Resolution of Discrepancies between Predicted and Measured in Situ WIPP Room Closures.* SAND88-2948, Sandia National Laboratories, Albuquerque, New Mexico.
13. Munson, D.E., 1998. Analysis of Multistage and Other Creep Data for Domal Salts, SAND98-2276, Sandia National Laboratories, Albuquerque, New Mexico.
14. Van Sambeek, L.L., J.L. Ratigan, & F.D. Hansen, 1993. Dilatancy of Rock Salt in Laboratory Tests, *Int. J. Rock Mech. Min. Sci. & Geomech. Abstr.* Vol. 30, No. 7, 735-738.